Characterizing the shape-morphing behaviour of 4D printed PLA structures

Author(s)

Georgantzinos, Stelios K.; Kostopoulos, Grigorios; Stamoulis, Konstantinos P.

DO

10.1088/1742-6596/2716/1/012034

Publication date

2024

Document Version

Final published version

Published in

Journal of Physics: Conference Series

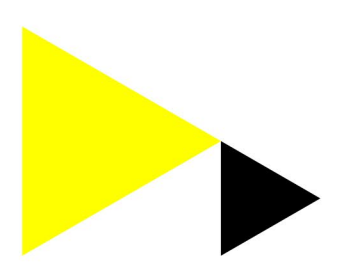
License

CC BY

Link to publication

Citation for published version (APA):

Georgantzinos, S. K., Kostopoulos, G., & Stamoulis, K. P. (2024). Characterizing the shape-morphing behaviour of 4D printed PLA structures. *Journal of Physics: Conference Series*, *2716*, Article 012034. https://doi.org/10.1088/1742-6596/2716/1/012034



General rights

It is not permitted to download or to forward/distribute the text or part of it without the consent of the author(s) and/or copyright holder(s), other than for strictly personal, individual use, unless the work is under an open content license (like Creative Commons).

Disclaimer/Complaints regulations

If you believe that digital publication of certain material infringes any of your rights or (privacy) interests, please let the Library know, stating your reasons. In case of a legitimate complaint, the Library will make the material inaccessible and/or remove it from the website. Please contact the library: https://www.amsterdamuas.com/library/contact, or send a letter to: University Library (Library of the University of Amsterdam and Amsterdam University of Applied Sciences), Secretariat, Singel 425, 1012 WP Amsterdam, The Netherlands. You will be contacted as soon as possible.

PAPER • OPEN ACCESS

Characterizing the shape-morphing behaviour of 4D printed PLA structures

To cite this article: Stelios K. Georgantzinos et al 2024 J. Phys.: Conf. Ser. 2716 012034

View the <u>article online</u> for updates and enhancements.

You may also like

- Hard magnetics and soft materials—a synergy
 P Narayanan, R Pramanik and A Arockiarajan
- Actuator placement optimization in an active lattice structure using generalized pattern search and verification Cosima Du Pasquier and Kristina Shea
- Plant-inspired adaptive structures and materials for morphing and actuation: a review Suyi Li and K W Wang



Joint Meeting of

The Electrochemical Society

•
The Electrochemical Society of Japan

•
Korea Electrochemical Society



Characterizing the shape-morphing behaviour of 4D printed PLA structures

Stelios K. Georgantzinos^{1,*}, Grigorios Kostopoulos¹, Konstantinos P. Stamoulis²

- ¹ Department of Aerospace Science and Technology, National and Kapodistrian University of Athens, 34400 Psachna, Greece
- ² Faculty of Technology, Amsterdam University of Applied Sciences, Rhijnspoorplein 2, 1091 GC Amsterdam, The Netherlands

Abstract. This study aims to provide an in-depth characterization of the intelligent behaviour exhibited by structures fabricated using fused deposition modelling (FDM) printing technology. The primary objective is to understand the variability in the shape-morphing behaviour of additively manufactured PLA structures. A comprehensive analysis is conducted to shed light on the impact of various factors on shape transformation, encompassing both working and printing parameters. To establish the relationship between the printing and working parameters with the shape morphing characteristics, the experimental procedure employs Taguchi's method design of experiments. Notably, the study quantitatively reveals the extent of these parameters' impact on the characteristics.

1. Introduction

4D printing, an evolution of the well-established 3D printing technology, introduces the dimension of time to the printing process [1]. Unlike traditional 3D printed objects that remain static post-production, 4D printed items can change their shape, properties, or functionalities over time in response to external stimuli such as temperature, light, or moisture. This dynamic behaviour is achieved using smart materials that can undergo controlled transformations [2-4].

In the aerospace industry, the potential applications of 4D printing are vast and transformative [5]. Aircraft and spacecraft components often operate under extreme conditions, from significant temperature fluctuations to varying atmospheric pressures. 4D printed components can be designed to adapt to these changes, ensuring optimal performance. For instance, wings or aerofoils that morph in response to aerodynamic conditions can lead to enhanced fuel efficiency and manoeuvrability [6]. Additionally, self-healing materials can significantly extend the lifespan of aerospace components, reducing maintenance costs and downtime. Furthermore, the lightweight nature of many 4D printed materials aligns with the aerospace industry's continuous pursuit of weight reduction, directly impacting fuel consumption and overall efficiency. As space exploration advances, the ability to print structures that can adapt to the space environment, or even self-assemble in space, becomes invaluable [7].

Shape morphing, at its core, refers to the ability of a material or structure to undergo controlled changes in its geometry or form in response to external stimuli [8-13]. This transformative capability is not simply a physical alteration; it represents a dynamic adaptation to environmental conditions, user requirements, or specific functionalities. Unlike traditional static structures, morphing structures can transition between multiple configurations, offering versatility and adaptability. The significance of shape morphing is profound, especially in the domain of advanced manufacturing and design. In environments where conditions are constantly changing, static designs may not always offer optimal

^{*} Corresponding author's e-mail: sgeor@uoa.gr

Content from this work may be used under the terms of the Creative Commons Attribution 3.0 licence. Any further distribution of this work must maintain attribution to the author(s) and the title of the work, journal citation and DOI.

Journal of Physics: Conference Series

2716 (2024) 012034 doi:10.1088/1742-6596/2716/1/012034

performance. Morphing structures, on the other hand, can adapt in real-time, ensuring that they always operate at their best. This adaptability can lead to enhanced efficiency, prolonged material lifespan, and even the creation of entirely new functionalities previously considered unreachable. As industries move towards more intelligent and responsive solutions, the concept of shape morphing emerges as a basis, covering the way for innovations that can respond to the world around them.

In the complex world of 4D printing, the final behaviour and characteristics of the printed structure are not solely determined by the material used but are also greatly influenced by numerous of working and printing parameters. These parameters, ranging from print speed, layer height, and nozzle diameter to temperature settings, infill density, and print orientation, play pivotal roles in determining the extent and nature of shape morphing [14,15]. For instance, a higher print speed might lead to different cooling rates, affecting the material's responsiveness to stimuli. Similarly, variations in infill patterns can result in structures with apparent flexibility and deformation characteristics [16]. The relations between these parameters can be complex, with each combination offering a unique set of morphing behaviours. Understanding and optimizing these parameters is essential, as they hold the key to unlocking the full potential of 4D printed structures, ensuring that they morph accurately, consistently, and predictably in their expected applications.

Although shape morphing in 4D printing has significant promise, realising its full potential requires an extensive and detailed comprehension of the relationships between the working and printing parameters. A wide range of shifting behaviours, some predictable and others less so, can result from the numerous combinations and interactions of these elements. This complexity emphasises why a thorough and methodical investigation is needed. The possibility of inconsistent or unexpected morphing results rises in the absence of such a planned approach, possibly undercutting the very benefits that 4D printing aims to provide. In addition to clarifying the complex correlations between factors, a methodical investigation opens the door for the creation of prediction models [17]. With the use of these models, engineers and designers can optimise parameters to achieve desired morphing results, ensuring repeatability, accuracy, and reliability in practical applications [18].

This work aims to characterise the shape-morphing behaviour of 4D printed Polylactic Acid (PLA) structures employing material extrusion technology, more especially the FDM technique, as we go deeper into the world of 4D printing. To prepare for the details of shape changes, we have utilised empirical analytical models that have been carefully developed based on solid experimental data, recognising the complexity inherent in this fundamental process. One of the main focuses of our study is the quantitative analysis, in which we try to determine how much different parameters affect the morphing properties. By using a holistic approach, we hope to provide insights that will advance the discipline and open up new possibilities for adaptable and responsive design.

2. Experimental Procedures

A new era of additively manufactured structures that may change their shape in response to environmental stimuli has begun with the introduction of 4D printing. These "intelligent" structures—which are mostly composed of PLA, the most well-known bio-sourced shape memory polymer—have drawn a lot of interest because of their potential uses in a variety of industries, from adaptive architecture to biomedical equipment. Research is still ongoing to determine how predictable and controllable their shape-morphing behaviour is. The final shape and behaviour of these structures are largely determined by the details of the printing process as well as the post-printing environment. This section explores every stage of the procedure, offering an in-depth overview of the variables impacting the development of these novel structures.

To gain a comprehensive understanding of the shape morphing in 4D-printed PLA structures, an extensive experimental methodology was developed. We aimed to capture the complex relationships among printing factors and the resulting morphing behaviours with this systematic strategy. The experimental characterisation procedure used in this study underlying the shape-morphing behaviour of 4D printed PLA structures is explained in detail in Figure 1. The procedure starts with the sample's design and slicing, which establishes the framework for the printing step that follows (Figure 1(a)). Next, utilising fused deposition modelling (FDM) technology, the sample is printed (Figure 1(b)). To ensure the stabilisation of its structure, the printed sample is cooled at room temperature for a certain

amount of time (Figure 1d). As part of the preparation for the activation phase, the sample must now be placed in a lab bath (Figure 1(d)). Figure 1(f) shows the sample's activation and deformation, demonstrating the sample's ability to change shape in response to external stimuli. The deformed sample is finally cooled to room temperature in Figure 1(g), where measurements and data are recorded. This comprehensive procedure ensures an in-depth understanding of the components influencing the printed structures' shape change.

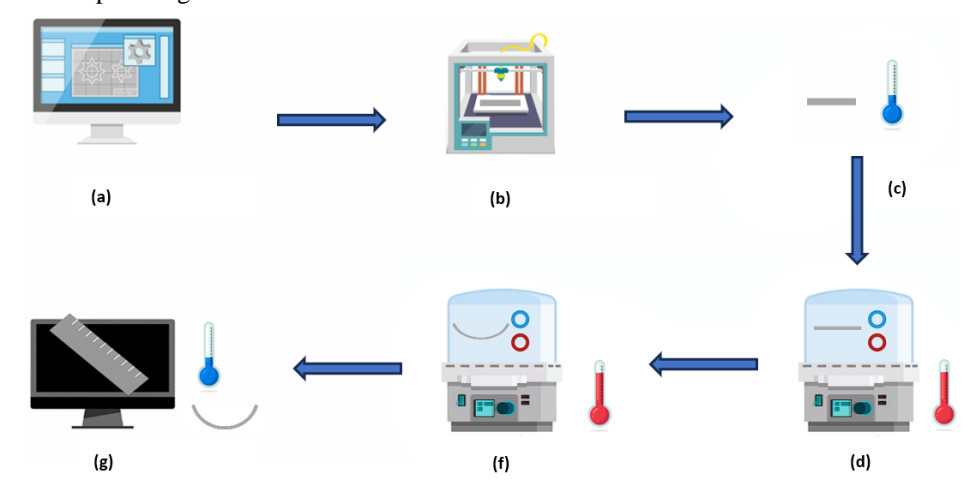


Figure 1. Experiment characterization process, (a) Design and slicing of the sample, (b) Printing of the sample, (c) Cooling down of the sample in room temperature, (d) Submergence of the sample within the laboratory bath, (f) Activation and deformation of the sample, (g) Cooling down of the deformed sample in room temperature, measurements, and data acquisition.

2.1. Materials and Equipment

The specimens used for conducting the experiments are of dimensions L = 70mm, b = 3.5 mm, and h = 1.5 mm. The process for producing the test specimens, from their original design stage in a Computer-Aided Design (CAD) environment to the physical 3D printed models with different layer heights, is thoroughly described in Figure 2. The process starts with the model shown in Figure 2(a), where the specimen is created using CAD software to ensure that its shape and dimensions are exact. The specimen is translated into the world of 3D printing after design, and a variety of printing parameters are defined in the slicing programme to provide the best print fidelity and performance. These parameters include, among others, print speed, bed and nozzle temperature, layer height, and layer width.

The subsequent segments of the figure present the tangible outcomes of these defined parameters. The model in Figure 2(b) showcases the specimen printed with a layer height of 0.1 mm, capturing the finest details and offering a smooth surface finish. The model in Figure 2(c) represents the specimen with a layer height of 0.2 mm, striking a balance between detail resolution and print duration. Concluding the series, the model in Figure 2(d) displays the specimen printed at a layer height of 0.3 mm, which, while being the quickest to produce, might present more visible layer lines. This array of models, each with its unique set of printing parameters, facilitates a comprehensive analysis, enabling researchers to discern the nuanced effects of each parameter on the final shape-morphing behaviour of the 4D printed structures.

The test specimens were fabricated using a K1 3D printer, a product of Creality from Shenzen Creality 3D Technology Co., Ltd. The chosen material for this effort was a premium-grade PLA filament, characterized by a diameter of 1.75 mm and a weight of 1.0 kg, in a pristine white shade, sourced from the Devil Design, a subsidiary of Devil Design Ryszka Mateja Sp. J., located in Mikołów, Poland. Following the precision-driven printing process, the specimens were subjected to experimental conditions using a laboratory water bath. This water bath, as shown in Figure 2(a), has the capacity to reach and sustain a particular target temperature, which is known as the activation temperature. The specimen's behaviour of changing its form begins by this temperature, which functions as an external

stimulus. Further along with this, Figure 2(b) shows the specialised equipment used for handling the test specimens properly. After that, the apparatus was carefully placed within the water bath to ensure that the experiments would proceed as easily as possible. Four minutes was the consistent exposure time to heat stimulation.

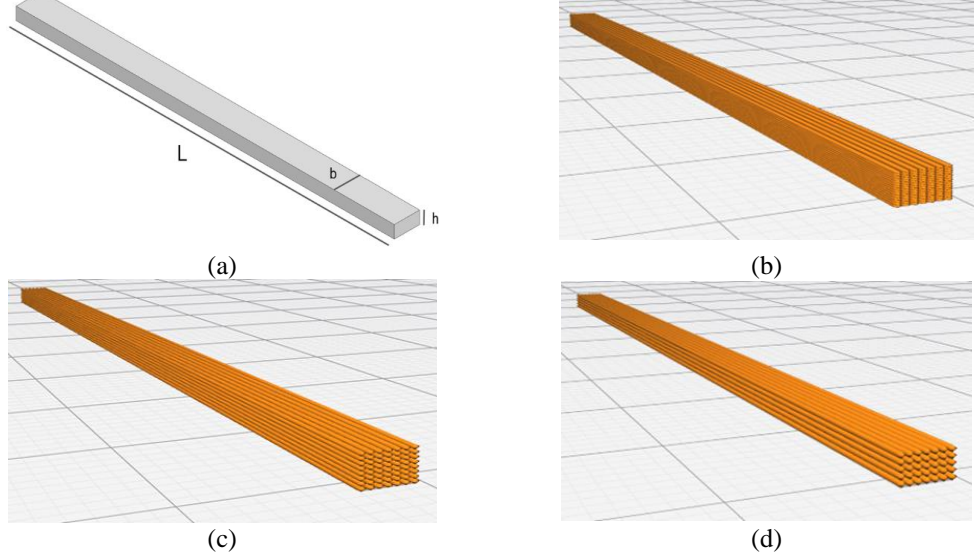
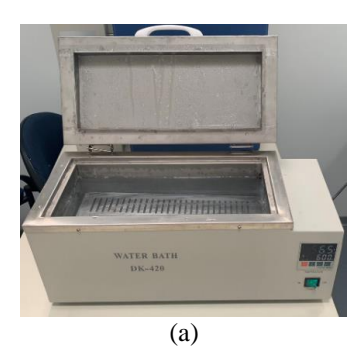


Figure 2. Designing the specimen in CAD and defining the printing parameters in the slicing software, (a) CAD model, (b) 3D printed model with layer height 0.1 mm, (c) 3D printed model with layer height 0.2 mm, (d) 3D printed model with layer height 0.3 mm.

2.2. Design of Experiments

We then proceed to an analysis that is carried out with the statistical software Minitab 17. Finding the effects of different printing factors, such as printing speed, layer height, flow rate, nozzle temperature, and bed temperature, together with the workings of the parameter, activation temperature, was our main goal. We used Taguchi's L18 Design of Experiments (DoE), an established methodology for its accuracy and efficiency, to accomplish this. The following is a detailed outline of the control parameters and their corresponding levels: There are six different levels of the activation temperature, expressed in degrees Celsius: 76°C, 80°C, 84°C, 88°C, 92°C, and 96°C. This range offers a complete spectrum for evaluating the material's behaviour under various thermal stimuli. There are three different degrees of printing speed, which are measured in millimetres per second: 50 mm/s, 80 mm/s, and 110 mm/s. These stages provide information about how the final printed structure is influenced by the deposition speed. A crucial factor in 3D printing is layer height, which is expressed in millimetres. There are three different levels for it: 0.1 mm, which represents accuracy and fine detail; 0.2 mm, which provides a balance between detail and print speed; and 0.3 mm, which tends to favour faster print times at the potential cost of surface smoothness. Finally, Layer Width is defined at three different levels: 0.36 mm, 0.4 mm, and 0.48 mm. It is likewise measured in millimetres. These levels assist in understanding how extrusion width affects the structural integrity and appearance of the printed object.

Using Taguchi's DoE was a strategic decision. Because of the dependence on orthogonal arrays, every parameter is given the same weight, enabling a fair assessment. This special characteristic makes sure that the presence or change of one parameter has no effect on the influence of another. Essentially, every element is independent, facilitating an open and unrestricted examination. The effectiveness of Taguchi's DoE is one of its main advantages. For example, the L18 array reduces the number of runs required for a full factorial design to just 18 compared to an extraordinary 1458 runs (or 6 x 3 x 3 x 3 x 3 x 3), which saves a great deal of time and cost.



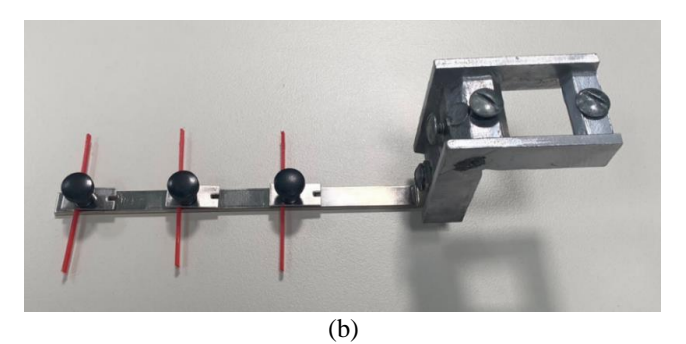


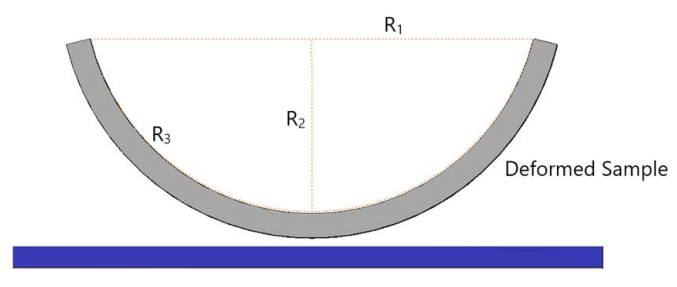
Figure 3. Experiment characterization process, (a) Design and slicing of the sample, (b) Printing of the sample, (c) Cooling down of the sample in room temperature, (d) Submergence of the sample within the laboratory bath, (f) Activation and deformation of the sample, (g) Cooling down of the deformed sample in room temperature, measurements, and data acquisition.

Table 1 provides a detailed summary of the experimental runs crafted using the Taguchi method. Within this table, the columns denote the control factors, the rows denote the individual runs (which are essentially combinations of factor levels), and each cell specifically represents the level of a factor for a specific run.

Table 1. The Taguchi L18 (6¹ x 3⁵) orthogonal array

Table 1. The Taguelli Lio (0 x 5) offingolial array						
Experiment	Activation	Printing	Layer	Layer	Nozzle	Bed
run	Temperature	Speed	Height	Width	Temperature	Temperature
	(°C)	(mm/s)	(mm)	(mm)	(°C)	(°C)
1	76	50	0.1	0.36	200	30
2	76	80	0.2	0.4	210	45
3	76	110	0.3	0.48	220	60
4	80	50	0.1	0.4	210	60
5	80	80	0.2	0.48	220	30
6	80	110	0.3	0.36	200	45
7	84	50	0.2	0.36	220	45
8	84	80	0.3	0.4	200	60
9	84	110	0.1	0.48	210	30
10	88	50	0.3	0.48	210	45
11	88	80	0.1	0.36	220	60
12	88	110	0.2	0.4	200	30
13	92	50	0.2	0.48	200	60
14	92	80	0.3	0.36	210	30
15	92	110	0.1	0.4	220	45
16	96	50	0.3	0.4	220	30
17	96	80	0.1	0.48	200	45
18	96	110	0.2	0.36	210	60

In the data acquisition phase, detailed measurements of R1, R2, and R3 were captured utilizing the advanced capabilities of the Autodesk Inventor Professional software. Analysing the deformed shape, R1 is identified as the chord of this deformed structure, representing the straight line connecting the two ends of the curve. R2 denotes the beam deflection, indicating the degree to which the beam deviates from its original position. Meanwhile, R3 represents the internal arc, capturing the curvature's essence within the deformed shape. A detailed visual depiction of these parameters can be further explored in Figure 4, providing a clearer understanding of their significance in the context of the deformation.



Printed Sample

Figure 4. Schematic representation of the deformed shape parameters, showcasing R1 as the chord connecting the two ends of the curve, R2 indicating the deflection, and R3 is the internal arc.

3. Results and discussion

The means and the Signal-to-Noise (S/N) ratios are calculated in order to evaluate the impact of each control component on the response. One robustness metric that is useful for identifying control factor settings that efficiently reduce noise is the S/N ratio. Minitab has four unique S/N ratios: "Smaller is better," "Larger is better," and two variants on "Nominal is best" [19]. These ratios are designed to meet varying response criteria. The 'Larger is better' (particularly for R2 responses) or 'Smaller is better' (primarily for R1 and R3 responses) criteria are used to determine the S/N ratio, depending on the individual responses.

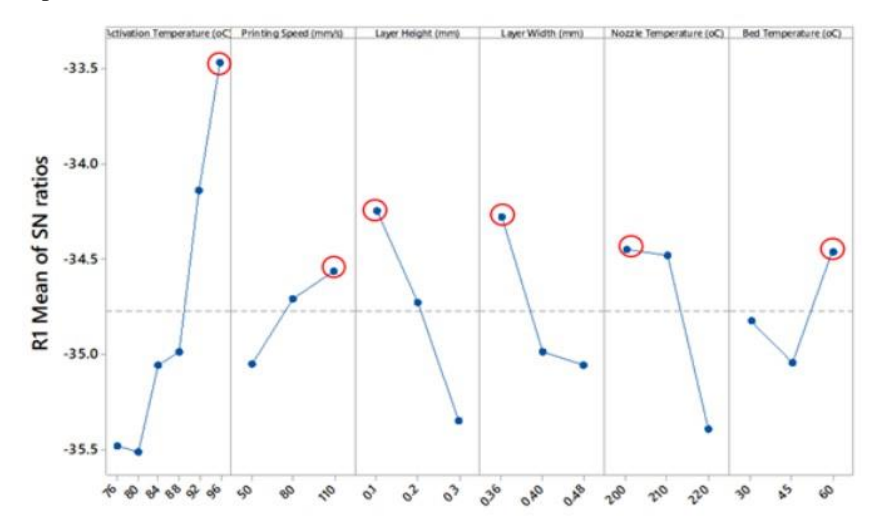


Figure 5. R1 Mean of SN ratios for each factor. Signal-to-noise: Smaller is better.

Improving the S/N ratio reduces the impact of noise elements and increases the desired feature [20]. The main goal of this study is to minimise the response (R1). For R1, a smaller value indicates a greater bending deformation, which aligns with our objective to minimize this response to achieve the desired flexibility in the printed structure. Figure 5 can be used to calculate the ideal levels of the process parameters. These ideal settings are shown by the levels that produce the highest S/N ratio results. Thus, level 6 (96°C) for the activation temperature, level 3 (110 mm/s) for the printing speed, level 1 (0.1 mm) for the layer height, level 1 (0.36) for the layer width, level 1 (200°C) for the nozzle temperature, and level 3 (60°C) for the bed temperature are the optimal settings.

Journal of Physics: Conference Series

2716 (2024) 012034 doi:10.1088/1742-6596/2716/1/012034

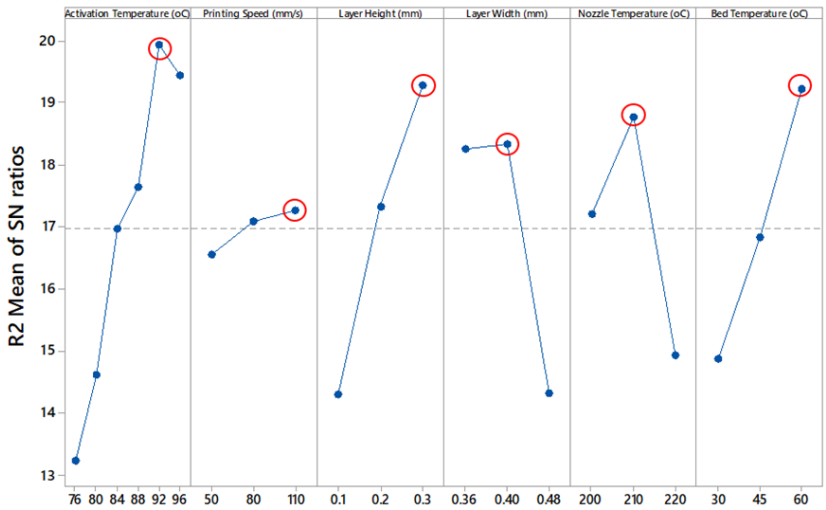


Figure 6. R2 Mean of SN ratios for each factor. Signal-to-noise: Larger is better.

The primary objective is to maximize the response (R2). For R2, a greater value corresponds to a greater bending deformation, which is desirable in our study. Hence, our objective to maximize this response is to enhance the structure's ability to bend as required by its intended application. To determine the optimal levels of the process parameters, one can refer to Figure 6. The levels yielding the highest Signal-to-Noise (S/N) ratio values indicate these optimal settings. Accordingly, the best settings are as follows: an activation temperature at level 5, equating to 92°C; a printing speed at level 3, translating to 110 mm/s; a layer height at level 3, which is 0.3 mm; a layer width at level 2, corresponding to 0.4 mm; a nozzle temperature at level 2, set at 210°C; and a bed temperature at level 3, calibrated to 60°C.

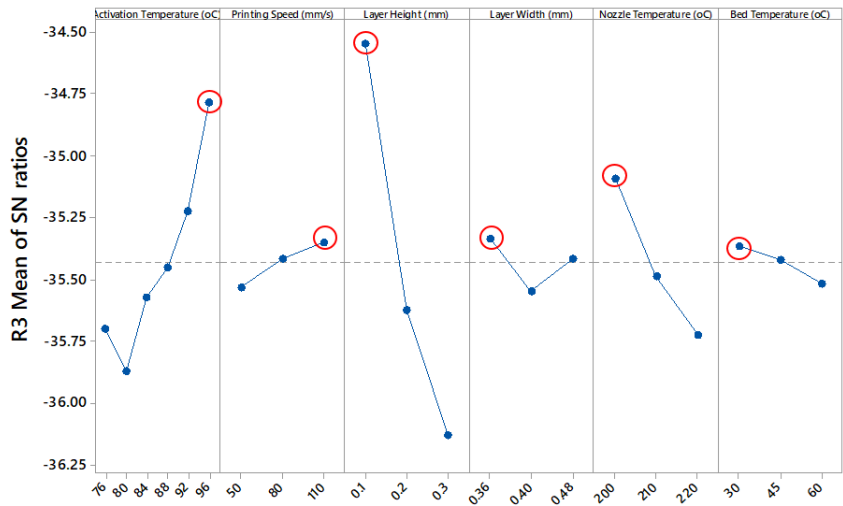


Figure 7. R3 Mean of SN ratios for each factor. Signal-to-noise: Smaller is better.

Furthermore, the primary goal is to minimize the response (R3). For R3, similarly to R1, a smaller value denotes a greater bending deformation. Our goal to minimize R3 is to ensure that the structure can achieve the necessary curvature without compromising its integrity. To ascertain the optimal levels of the process parameters, one can consult Figure 7. The levels that yield the highest Signal-to-Noise (S/N) ratio values pinpoint these optimal configurations. Based on this, the ideal settings are: an activation temperature at level 6, which corresponds to 96° C; a printing speed at level 3, equivalent to 110 mm/s; a layer height at level 1, set at 0.1 mm; a layer width at level 1, measuring 0.36 mm; a nozzle temperature at level 1, calibrated to 200° C; and a bed temperature at level 1, adjusted to 30° C.

Journal of Physics: Conference Series

2716 (2024) 012034 doi:10.1088/1742-6596/2716/1/012034

4. Conclusions

The field of additively created structures has expanded its boundaries with the introduction of 4D printing. These structures mark a major advancement in the field of intelligent design since they can dynamically change their shape in response to external stimuli. They are mostly made of PLA, and they have a wide range of potential uses, from creative biomedical treatments to flexible aircraft parts. Nevertheless, it is still difficult to achieve a consistent and predictable shape-morphing behaviour, with post-printing circumstances and the complexities of the printing process playing crucial roles.

We carefully followed every stage of our research process, from the first idea for the design to the final printed product. Based on Taguchi's L18 DoE, the experimental design provided an organised method for comprehending the subtle impacts of different printing factors on morphing behaviours. We identified the best configurations for various reactions using this methodical approach, revealing the crucial roles of factors like layer height, printing speed, activation temperature, and nozzle temperature. The experimental results are currently being further analysed in order to forecast acceptable shapemorphing capabilities or to develop ideal 4D printed structures.

To sum up, our study has enhanced our knowledge of 4D-printed PLA structures and provided the groundwork for more research in this area. We can better utilise the revolutionary potential of 4D printing by identifying the optimum parameter settings. In the future, even more innovative possibilities are provided by the developing idea of 6D printing [21]. 6D printing is a novel branch of additive manufacturing that expands upon 4D and 5D printing techniques. It involves a process that utilizes five degrees of freedom to create an object (5D printing), which is then capable of changing its shape or properties in response to environmental stimuli. The term '6D printing' is introduced to describe the production of smart/intelligent material components that are not only structurally more effective and material-efficient but also capable of performing movements and potentially reconfiguring themselves in response to external stimuli, as predicted by mathematical modeling and simulations.

5. References

- [1] Momeni F, Liu X and Ni J 2017 Mater. Des. 122 42
- [2] Choi J, Kwon O, Jo W, Lee H and Moon M 2015 3D Print. Addit. Manuf. 2 159
- [3] Shin D, Kim T and Kim D 2017 Int. J. Precis. Eng. Manuf. Green Technol. 4 349
- [4] Pei E and Loh G 2018 Prog. Addit. Manuf. 3 95
- [5] Ntouanoglou K, Stavropoulos P and Mourtzis D 2018 Procedia Manuf. 18 120
- [6] Sri Harsha A and Vikram Kumar C 2021 Int. J. Eng. 34 272
- [7] Wan X, Luo L, Liu Y and Leng J 2020 Adv. Sci. 7 2001000.
- [8] Alapan Y, Karacakol A, Guzelhan S, Isik I and Sitti M 2020 Sci. Adv. 6 eabc6414
- [9] Sofla A, Meguid S, Tan K and Yeo W 2010 Mater. Des. 31 1284
- [10] Neville R, Scarpa F and Pirrera A 2016 Sci. Rep. 6 31067
- [11] Rodriguez J, Zhu C, Duoss E, Wilson T, Spadaccini C and Lewicki J 2016 Sci. Rep. 6 27933
- [12] Bastola A and Hossain M 2021 Mater. Des. 211 110172
- [13] Rogkas N, Vakouftsis C, Spitas V, Lagaros N and Georgantzinos S 2022 Micromachines 13 775
- [14] Wang J, Wang Z, Song Z, Ren L, Liu Q and Ren L 2019 Adv. Mater. Technol. 4 1900535
- [15] Barletta M, Gisario A and Mehrpouya, M 2021 J. Manuf. Process. 61 473
- [16] Lubombo C and Huneault M 2018 Mater. Today Commun. 17 214
- [17] Biswas M, Chakraborty S, Bhattacharjee A and Mohammed Z 2021 *Adv. Funct. Mater.* **31** 2100257.
- [18] Sossou G, Demoly F, Belkebir H, Qi H, Gomes S and Montavon G 2019 Mater. Des. 181 108074.
- [19] Bilga P, Singh S and Kumar R 2016 J. Clean. Prod. 137 1406
- [20] Salehi M, Saadatmand M and Mohandesi J 2012 Trans. Nonferrous Met. Soc. 22 1055
- [21] Georgantzinos S, Giannopoulos G and Bakalis P 2021 J. Compos. Sci. 5 119